

An expanding radio nebula produced by a giant flare from the magnetar SGR 1806–20

B. M. Gaensler,¹ C. Kouveliotou,² J. D. Gelfand,¹ G. B. Taylor,^{3,4} D. Eichler,⁵ R. A. M. J. Wijers,⁶ J. Granot,³ E. Ramirez-Ruiz,⁷ Y. E. Lyubarsky,⁵ R. W. Hunstead,⁸ D. Campbell-Wilson,⁸ A. J. van der Horst,⁶ M. A. McLaughlin,⁹ R. P. Fender,¹⁰ M. A. Garrett,¹¹ K. J. Newton-McGee,^{8,12} D. M. Palmer,¹³ N. Gehrels¹⁴ and P. M. Woods¹⁵

¹ Harvard-Smithsonian Center for Astrophysics, 60 Garden Street, Cambridge, MA 02138, USA

² NASA / Marshall Space Flight Center, NSSTC, XD-12, 320 Sparkman Drive, Huntsville, AL 35805, USA

³ Kavli Institute for Particle Astrophysics and Cosmology, Stanford University, P.O. Box 20450, Stanford, CA 94309, USA

⁴ National Radio Astronomy Observatory, P.O. Box O, Socorro, NM 87801, USA

⁵ Department of Physics, Ben Gurion University, POB 653, Beer Sheva 84105, Israel

⁶ Astronomical Institute “Anton Pannekoek”, University of Amsterdam, Kruislaan 403, 1098 SJ, Amsterdam, The Netherlands

⁷ Institute for Advanced Study, Einstein Drive, Princeton, NJ 08540, USA

⁸ School of Physics, University of Sydney, NSW 2006, Australia

⁹ University of Manchester, Jodrell Bank Observatory, Macclesfield, Cheshire SK11 9DL, UK

¹⁰ School of Physics and Astronomy, University of Southampton, Highfield, Southampton SO17 1BJ, UK

¹¹ Joint Institute for VLBI in Europe, Postbus 2, 7990 AA Dwingeloo, The Netherlands

¹² Australia Telescope National Facility, CSIRO, PO Box 76, Epping, NSW 1710, Australia

¹³ Los Alamos National Laboratory, P.O. Box 1663, Los Alamos, NM 87545, USA

¹⁴ NASA / Goddard Space Flight Center, Code 661, Greenbelt, MD 20771, USA

¹⁵ Universities Space Research Association, NSSTC, XD-12, 320 Sparkman Drive, Huntsville, AL 35805, USA

Soft gamma repeaters (SGRs) are “magnetars”, a small class of slowly spinning neutron stars with extreme surface magnetic fields, $B \sim 10^{15}$ gauss.^{1–3} On 2004 December 27, a giant flare⁴ was detected from the magnetar SGR 1806–20,² the third such event ever recorded.^{5,6} This burst of energy was detected by a variety of instruments^{7,8} and even caused an ionospheric disturbance in the Earth’s upper atmosphere recorded around the globe.⁹ Here we report the detection of a fading radio afterglow produced by this outburst, with a luminosity 500 times larger than the only other detection of a similar source.¹⁰ From day 6 to day 19 after the flare from SGR 1806–20, a resolved, linearly polarized, radio nebula was seen, expanding at approximately a quarter the speed of light. To create this nebula, at least 4×10^{43} ergs of energy must have been emitted by the giant flare in the form of magnetic fields and relativistic particles. The combination of spatially resolved structure and rapid time evolution allows a study in unprecedented detail of a nearby analog to supernovae and gamma-ray bursts.

Almost seven days after the 2004 Dec. 27 giant flare, we observed SGR 1806–20 with the Very Large Array (VLA) in its highest resolution configuration (maximum baseline length 36.4 km). We identified a

bright but fading radio source designated VLA J180839–202439 (see Fig. 1), whose position was consistent with the previously reported localization¹¹ of the SGR. This close juxtaposition, plus the transient nature of the emission, makes it certain that VLA J180839–202439 is the radio afterglow of the giant flare from SGR 1806–20. For a distance¹² to SGR 1806–20 of $15d_{15}$ kiloparsecs, the 1.4-GHz flux density of this source at first detection implies an isotropic spectral luminosity of $5d_{15}^2 \times 10^{15}$ W Hz⁻¹, approximately 500 times larger than the radio afterglow seen from SGR 1900+14 after a giant flare in 1998.¹⁰ No other magnetar has been detected in the radio band, either in quiescence or during active periods.^{13,14}

Given the very bright nature of this afterglow, we organized an international campaign over a broad range of frequencies, 0.35 to 16 GHz, to track the decay of the radio emission of VLA J180839–202439. Here we present a subset of these observations, made on days 6 to 19 after the giant flare, consisting of images made using the VLA, the Australia Telescope Compact Array (ATCA), the Westerbork Synthesis Radio Telescope (WSRT) and the Molonglo Observatory Synthesis Telescope (MOST) (see Supplementary Methods for further information).

Figure 2 shows the combined light curves from these four telescopes covering the frequency range 0.84 to 8.5 GHz. These data are consistent with a sudden increase in the decay rate at day 8.8, as summarised in Table 1 and shown by the linear fits in Figure 2. Specifically, if we assume that $S_\nu \propto t^\delta$ (where S_ν is the flux density at frequency ν), after day 8.8 we find an achromatic and rapid decline, $\delta \approx -2.7$, in six independent frequency bands (a similarly rapid decline was also observed¹⁰ for the radio afterglow of SGR 1900+14 in 1998). After carefully accounting for the instrumental response of the VLA antennas we find that VLA J180839–202439 is significantly linearly polarized (see Fig. 3), which indicates that the emission mechanism is synchrotron radiation. In our earliest observations this emission was already optically thin, but showed clear evidence for a spectral steepening at high frequencies (see caption to Fig. 2). From day 11.2 onward, the spectrum was consistent with an unbroken power law from 0.84 to 8.5 GHz with $\alpha = -0.75 \pm 0.02$ (where $S_\nu \propto \nu^\alpha$), again similar to the 1998 afterglow of SGR 1900+14. This implies a power-law energy distribution of the emitting electrons, $dN/dE \propto E^{-p}$, with $p = 1 - 2\alpha = 2.50 \pm 0.04$.

Our highest resolution measurements are those made with the VLA at 8.5 GHz. The visibility data from these observations, as shown for one epoch in Figure 1, demonstrate that VLA J180839–202439 is resolved. A Gaussian is a good fit to the visibilities at each epoch, with no significant persistent residuals (forthcoming higher resolution images from the VLBA and MERLIN will test the validity of this model). Figure 3 demonstrates that from day 6.9 to day 19.7, the data were consistent with constant isotropic expansion since outburst at a speed $v/c = (0.27 \pm 0.10)d_{15}$, with no noticeable deceleration as of day 19.7. Other than in one observation at day 16.8, the source was significantly elliptical, with an axial ratio ~ 0.6 and with the major axis oriented $\approx 60^\circ$ west of north.

The spectrum and angular size of VLA J180839–202439 allow us to apply standard equipartition arguments for synchrotron sources,¹⁵ implying a minimum magnetic field $B_{\min} = 0.02d_{15}^{-2/7}[(1 + \kappa)F_{100}/f]^{2/7}\theta_{50}^{-6/7}$ gauss, where $100F_{100}$ mJy is the flux density of VLA J180839–202439 at 1.4 GHz, κ

the ratio of the energy in heavy particles to that in electrons, f is the volume filling factor of magnetic fields and relativistic particles, and $50\theta_{50}$ mas is the source’s angular diameter. The minimum energy in particles and magnetic fields in the emitting region is $E_{\min} = 4 \times 10^{43} d_{15}^{17/7} [(1 + \kappa)F_{100}]^{4/7} f^{3/7} \theta_{50}^{9/7}$ ergs. The spectra show no evidence of self-absorption at frequencies above 0.6 GHz at early times,¹⁶ which is consistent with these parameters provided that the emitting medium has a density $n_0 \lesssim 0.1f \text{ cm}^{-3}$. We can derive an additional independent energy estimate because of this rare opportunity to measure the expansion velocity directly. From the constant expansion speed observed over the first 20 days, we infer $E_{\min} \approx 6 \times 10^{42} \Omega (n_0/0.01 \text{ cm}^{-3})(v/0.27c)^5$ ergs, where Ω is the opening solid angle of the ejected material.

Giant flares from magnetars are thought to result from shearing and reconnection of the extreme magnetic fields near the neutron star surface.^{17,18} The inferred minimum energy in the radio nebula is somewhat smaller than the emitted gamma-ray energy,^{7,8} but is much larger than the electron/positron pair luminosity that would be expected to survive annihilation close to the magnetar. This suggests that baryons may have been ablated off the surface by the intense illumination of the flaring magnetosphere.^{17,18} The radio nebula could be naturally created by these baryons, which move off the magnetar at high velocity, $\gtrsim 0.5c$, and then shock the ambient medium.

The very steep decay of the radio emission after day 8.8, $\delta \approx -2.7$, combined with the observed subluminal expansion velocity of VLA J180839–202439, is difficult to produce in standard gamma-ray burst blast-wave models.^{19–21} The light curves may thus represent an adiabatically expanding population of electrons accelerated at a particularly active phase, such as might occur if the ejecta collided with a pre-existing shell. Such a shell is naturally made by SGR 1806–20 itself, since its quiescent wind²² of luminosity²³ $\sim 10^{34} \text{ ergs s}^{-1}$ will sweep up a bow shock^{24,25} of stand-off distance $\sim 10^{16} \text{ cm}$ (corresponding to an angular extent $\sim 40d_{15}^{-1}$ mas) as it moves through the interstellar medium (ISM) at a typical neutron star velocity²⁶ of $\sim 200 \text{ km s}^{-1}$. The star’s motion creates a cigar-shaped cavity, mostly as a wake that trails the bow shock. If this pre-existing shell is hit by $\sim 10^{43}$ – 10^{44} ergs of energy from the SGR’s giant flare, it will be shocked and swept outward, resulting in a violent episode of particle acceleration that puts much of the energy into a steadily expanding synchrotron-emitting shell 4 to 8 days after the giant flare. If we suppose that this shell maintains constant thickness and constant expansion speed, then its volume, V , increases as t^2 , and the magnetic field will decay as $V^{-1/2}$ if directed within the tangent plane of the shell ($V^{-2/3}$ if tangled in three dimensions). This predicts a power law index for the radio decay $\delta = (7\alpha - 3)/3 = -2.75 \pm 0.05$ (for $B \propto V^{-1/2}$) or $\delta = (8\alpha - 4)/3 = -3.33 \pm 0.05$ (for $B \propto V^{-2/3}$), consistent with the steep decay observed here. The overall evolution can be complicated by the fact that the ejecta may be somewhat collimated, and may hit the shell at different places and times — we defer detailed modelling to later papers, pending higher resolution images from MERLIN and the VLBA.

At early times, the polarization position angle on the sky is approximately perpendicular to the axis of the radio source (see Fig. 3), suggesting that the magnetic field in the emitting plasma (on average) is aligned preferentially along this axis. This is consistent with the shock producing a preferred magnetic anisotropy

in the shock plane. Between observations at days 11.0 and 13.7 the polarized fraction and polarization angle both changed noticeably and a possible bump in the 1.4-GHz light curve is apparent; at day 16.8, the position angle of the major axis of the source also changed considerably. These results suggest that a different part of the outflow may have assumed the dominant role in the emission, as can occur if one region fades faster than another.

The intensity of this radio afterglow confirms the conservative inference made from the X- and gamma-ray detections^{7,8} that this event was $\gtrsim 2$ orders of magnitude more energetic than the 1998 giant flare from SGR 1900+14. It is difficult to attribute the difference to beaming effects, because the measured expansion velocity ($\sim 0.3c$) appears to be modest. A release of $> 10^{46}$ ergs in a single magnetar flare^{7,8} suggests that a rather large fraction, ~ 10 percent, of the total magnetic energy can be released at once. Continued measurements of the morphology of the expanding radio source can provide an indication of whether the energy release took place at a specific location on the star's surface, or was a truly global phenomenon that rearranged the crust or even the entire interior.

Received 18 January, 2005; Accepted 17 February, 2005.

1. Duncan, R. C. & Thompson, C. Formation of very strongly magnetized neutron stars: Implications for gamma-ray bursts. *ApJ* **392**, L9–L13 (1992).
2. Kouveliotou, C. et al. An X-ray pulsar with a superstrong magnetic field in the soft γ -ray repeater SGR 1806–20. *Nature* **393**, 235–237 (1998).
3. Woods, P. M. & Thompson, C. in *Compact Stellar X-ray Sources* (eds Lewin, W. H. G. & van der Klis, M.) (Cambridge University Press, Cambridge, 2004). in press (astro-ph/0406133).
4. Borkowski, J., Gotz, D., Mereghetti, S., Mowlavi, N., Shaw, S. & Turler, M. Giant flare from SGR 1806–20 detected by *INTEGRAL*. *GCN Circular* No. 2920 (2004).
5. Mazets, E. P., Golenetskii, S. V., Ilinskii, V. N., Apetkar, R. L. & Guryan, Y. A. Observations of a flaring X-ray pulsar in Dorado. *Nature* **282**, 587–589 (1979).
6. Hurley, K. et al. A giant periodic flare from the soft gamma repeater SGR 1900+14. *Nature* **397**, 41–43 (1999).
7. Palmer, D. M. et al. *Swift* observation of a giant flare from magnetar SGR 1806–20. *Nature*, (2005). submitted.
8. Hurley, K. et al. A tremendous flare from SGR 1806–20 with implications for short-duration gamma-ray bursts. *Nature*, (2005). submitted.
9. Campbell, P. et al. SGR1806: Detection of a sudden ionospheric disturbance. *GCN Circular* No. 2932 (2005).
10. Frail, D. A., Kulkarni, S. R. & Bloom, J. S. An outburst of relativistic particles from the soft gamma-ray repeater SGR 1900+14. *Nature* **398**, 127–129 (1999).
11. Kaplan, D. L., Fox, D. W., Kulkarni, S. R., Gotthelf, E. V., Vasisht, G. & Frail, D. A. Precise *Chandra* localization of the soft gamma-ray repeater SGR 1806-20. *ApJ* **564**, 935–940 (2002).
12. Corbel, S. & Eikenberry, S. S. The connection between W31, SGR 1806–20, and LBV 1806–20: Distance, extinction, and structure. *A&A* **419**, 191–201 (2004).

13. Lorimer, D. R. & Xilouris, K. M. PSR J1907+0918: A young radio pulsar near SGR 1900+14 and G42.8+0.6. *ApJ* **545**, 385–389 (2000).
14. Kouveliotou, C. et al. Multiwavelength observations of the soft gamma repeater SGR 1900+14 during its 2001 April activation. *ApJ* **558**, L47–L50 (2001).
15. Pacholczyk, A. G. *Radio Astrophysics*. Freeman San Francisco (1970).
16. Chandra, P. SGR 1806–20: Further low frequency GMRT results. *GCN Circular* No. 2947 (2005).
17. Thompson, C. & Duncan, R. C. The giant flare of 1998 August 27 from SGR 1900+14. II. Radiative mechanism and physical constraints on the source. *ApJ* **561**, 980–1005 (2001).
18. Thompson, C. & Duncan, R. C. The soft gamma repeaters as very strongly magnetized neutron stars. I. Radiative mechanism for outbursts. *MNRAS* **275**, 255–300 (1995).
19. Rhoads, J. E. The dynamics and light curves of beamed gamma-ray burst afterglows. *ApJ* **525**, 737–749 (1999).
20. Granot, J., Piran, T. & Sari, R. Images and spectra from the interior of a relativistic fireball. *ApJ* **513**, 679–689 (1999).
21. Cheng, K. S. & Wang, X. Y. The radio afterglow from the giant flare of SGR 1900+14: The same mechanism as afterglows from classic gamma-ray bursts? *ApJ* **593**, L85–L88 (2003).
22. Thompson, C., Duncan, R. C., Woods, P. M., Kouveliotou, C., Finger, M. H. & van Paradijs, J. Physical mechanisms for the variable spin-down and light curve of SGR 1900+14. *ApJ* **543**, 340–350 (2000).
23. Woods, P. M., Kouveliotou, C., Göğüş, E., Finger, M. H., Swank, J., Markwardt, C. B., Hurley, K. & van der Klis, M. Large Torque Variations in Two Soft Gamma Repeaters. *ApJ* **576**, 381–390 (2002).
24. Wilkin, F. P. Exact analytic solutions for stellar wind bow shocks. *ApJ* **459**, L31–L34 (1996).
25. Gaensler, B. M., Jones, D. H. & Stappers, B. W. An optical bow shock around the nearby millisecond pulsar J2124–3358. *ApJ* **580**, L137–L141 (2002).
26. Arzoumanian, Z., Chernoff, D. F. & Cordes, J. M. The velocity distribution of isolated radio pulsars. *ApJ* **568**, 289–301 (2002).
27. Staveley-Smith, L., Manchester, R. N., Kesteven, M. J., Tzioumis, A. K. & Reynolds, J. E. Structure in the radio remnant of Supernova 1987A. *Proc. Astr. Soc. Aust.* **10**, 331–334 (1993).
28. Brown, J. C., Taylor, A. R. & Jackel, B. J. Rotation measures of compact sources in the Canadian Galactic Plane Survey. *ApJS* **145**, 213–223 (2003).

Supplementary Information accompanies the paper on www.nature.com/nature.

Correspondence and requests for materials should be addressed to B.M.G. (bgaensler@cfa.harvard.edu).

Acknowledgements

We thank Jim Ulvestad, Joan Wrobel, Bob Sault, Tony Foley and Rene Vermeulen for rapid scheduling of the VLA, ATCA and WSRT; Tracey DeLaney, Ger de Bruyn and Crystal Brogan for assistance with data analysis; and

Dick Manchester, Dale Frail and Mark Wieringa for help with the observations. NRAO is a facility of the NSF operated under cooperative agreement by AUI. The Australia Telescope is funded by the Commonwealth of Australia for operation as a National Facility managed by CSIRO. The MOST is operated by the University of Sydney and supported in part by grants from the ARC. The WSRT is operated by ASTRON with financial support from NWO. B.M.G. acknowledges the support of NASA through a Long Term Space Astrophysics grant. D.E. acknowledge support from the Israel-U.S. BSF, the ISF, and the Arnow Chair of Physics. Y.L. acknowledges support from the German-Israeli Foundation. R.A.M.J.W and A.J.H. acknowledge support from NWO.

FIGURE & TABLE CAPTIONS

TABLE 1: The rate of decay of the radio emission from VLA J180839–202439 at six independent frequencies. At each frequency, ν , it has been assumed that the radio flux density decays as $S_\nu \propto t^{\delta_\nu}$, with a break in the power law index, δ_ν , at time t_0 . To determine values of t_0 and δ_ν , a weighted least squares fit of a broken power law has been applied to each data-set, with t_0 a free parameter. In each case, the fit shown is the only local minimum in χ^2 which meets the requirements that there are at least two data-points on either side of the break, the change in temporal index on either side of the break is larger than its uncertainties, and the power-law fits on either side of the break meet at the break point. Before day 8.8, we find that δ_ν possibly decreases with ν ; after day 8.8, the flux decays rapidly at all frequencies with a power-law index $\delta \approx -2.7$, independent of ν .

FIGURE 1: Radio emission from VLA J180839–202439 at 8.5 GHz. The main panel shows the visibility amplitude as a function of projected baseline length (in units of thousands of wavelengths; $100 \text{ k}\lambda \approx 3.5$ kilometers) at epoch 2005 Jan 06.8 (9.9 days after the giant flare), as seen by the VLA. The data have been self-calibrated in phase until the solution converged, and each baseline has then been time-averaged over the entire observation of duration 40 minutes. The error bars show the standard error in the mean of the amplitude on each baseline. The decrease in amplitude as a function of increasing baseline length clearly indicates that the source is resolved. The inset shows the image of the source at three epochs, smoothed to a uniform resolution of $0''.5$ (indicated by the green circle at lower right). The origin of the coordinate axes is the position of SGR 1806–20 measured with the *Chandra X-ray Observatory*,¹¹ which has an uncertainty of $0''.3$ in each coordinate. The false-colour representation is on a linear scale, ranging from -0.3 to the peak brightness of 53 mJy beam^{-1} . The contours are drawn at levels of 20%, 40%, 60% and 80% of this peak. No source is seen in archival 8.5-GHz data from 1994 March, down to a $5\text{-}\sigma$ upper limit of 0.1 mJy . In the days after the giant flare, a bright but rapidly fading source is now seen at this position. The precise location of VLA J180839–202439 was determined by phase referencing to several nearby calibrators with well-determined positions. Our best measurement was on Jan. 16.6, for which we measured a position for VLA J180839–202439 (equinox J2000) of Right Ascension (R.A.) $18^{\text{h}}08^{\text{m}}39^{\text{s}}.343 \pm 0^{\text{s}}.002$, Declination (Dec.) $-20^{\circ}24'39''.80 \pm 0''.04$. The source’s proper motion over the time span presented in this paper is $-2.8 \pm 6.5 \text{ mas day}^{-1}$ in R.A. and $-2.2 \pm 6.5 \text{ mas day}^{-1}$ in Dec.

FIGURE 2: Time evolution of the radio flux density from VLA J180839–202439. The x-axis indicates days since the giant flare was detected from SGR 1806–20, on 2004 Dec 27.90 UT. The radio data originate from ATCA, MOST and WSRT measurements made in six independent frequency bands. Each symbol represents a different telescope, while each colour indicates a different frequency. Measurement uncertainties

are indicated at the $1\text{-}\sigma$ level. Fits to the data are indicated by dashed lines, and represent the results of applying the broken power-law model described in Table 1 to the data. Significant deviations from this fit are seen at both 1.4 and 2.4 GHz, suggesting short-term time-variability in the source (most notably the possible “bump” in the 1.4 GHz light curve seen with multiple telescopes on days 10–11 after the flare). These data also allow us to compute the evolution of the radio spectral index, α (defined as $S_\nu \propto \nu^\alpha$). At three epochs with good frequency coverage between 8.4 and 9.9 days after the flare, there is clear evidence for a spectral break, from $\alpha \approx -0.66$ below ~ 5 GHz to $\alpha \approx -1.0$ above. Other data cannot rule out this break being present from day 6.9 (when the source was first detected) through to day 11.0. From day 11.2 onward, the spectrum has been consistent with an unbroken power law from 0.84 to 8.5 GHz with $\alpha = -0.75 \pm 0.02$.

In addition to the data shown here, on 2004 December 29, we used the Parkes Radio Telescope at 1.4 GHz to search for radio pulsations from SGR 1806–20. For dispersion measures in the range 0 to 2000 parsecs cm^{-3} , we found no pulsed signal at or near the star’s X-ray period² of 7.5 sec down to a level of ≈ 0.2 mJy (these data provide no constraint on the unpulsed flux).

FIGURE 3: Structural and polarization properties of VLA J180839–202439 as a function of time, as seen with the VLA at 8.5 GHz. The x-axis indicates days since the giant flare. The uppermost panel plots the radius of the source, determined by modelling²⁷ the visibilities at each epoch as a two-dimensional Gaussian function in the Fourier plane of arbitrary position, amplitude, diameter, axial ratio and orientation, and then taking the geometric mean of the semi-major and semi-minor axes. The broken line shows a weighted linear least squares fit to the data. The indicated expansion velocity assumes two-sided or isotropic expansion at a distance of 15 kiloparsecs. The two panels below this show the axial ratio and position angle (measured north through east) of this best-fit Gaussian at each epoch. The fourth panel shows the fractional linear polarization of VLA J180839–202439 at 8.5 GHz. We find that the position angle of this linearly polarized emission is a linear function of ν^{-2} at each epoch, indicating the presence of Faraday rotation from foreground magnetised plasma. We measure a Faraday rotation measure (RM) of $+272 \pm 10$ rad m^{-2} at multiple epochs, similar to the value $\text{RM} = +290 \pm 20$ rad m^{-2} obtained for the adjacent calibrator, MRC B1817–254, and typical of RMs seen through the Galactic plane.²⁸ Any contribution to the RM from the immediate environment of the magnetar must thus be small. The fifth panel shows the position angle of the electric field vector of linear polarization from VLA J180839–202439 after correction for this foreground Faraday rotation. Uncertainties at the $1\text{-}\sigma$ level are indicated for all data.

Table 1.

ν (GHz)	t_0 (days)	$\delta_\nu (t < t_0)$	$\delta_\nu (t > t_0)$
0.84	≤ 10.2	...	-2.7 ± 0.8
1.4	$9.0^{+0.4}_{-0.6}$	-1.6 ± 0.2	-2.61 ± 0.09
2.4	≤ 9.0	...	-2.74 ± 0.07
4.8	$8.8^{+0.2}_{-0.4}$	-1.5 ± 0.1	-2.84 ± 0.08
6.1	≤ 11.3	...	-2.6 ± 0.2
8.5	$8.8^{+0.2}_{-0.4}$	-2.2 ± 0.2	-2.54 ± 0.04

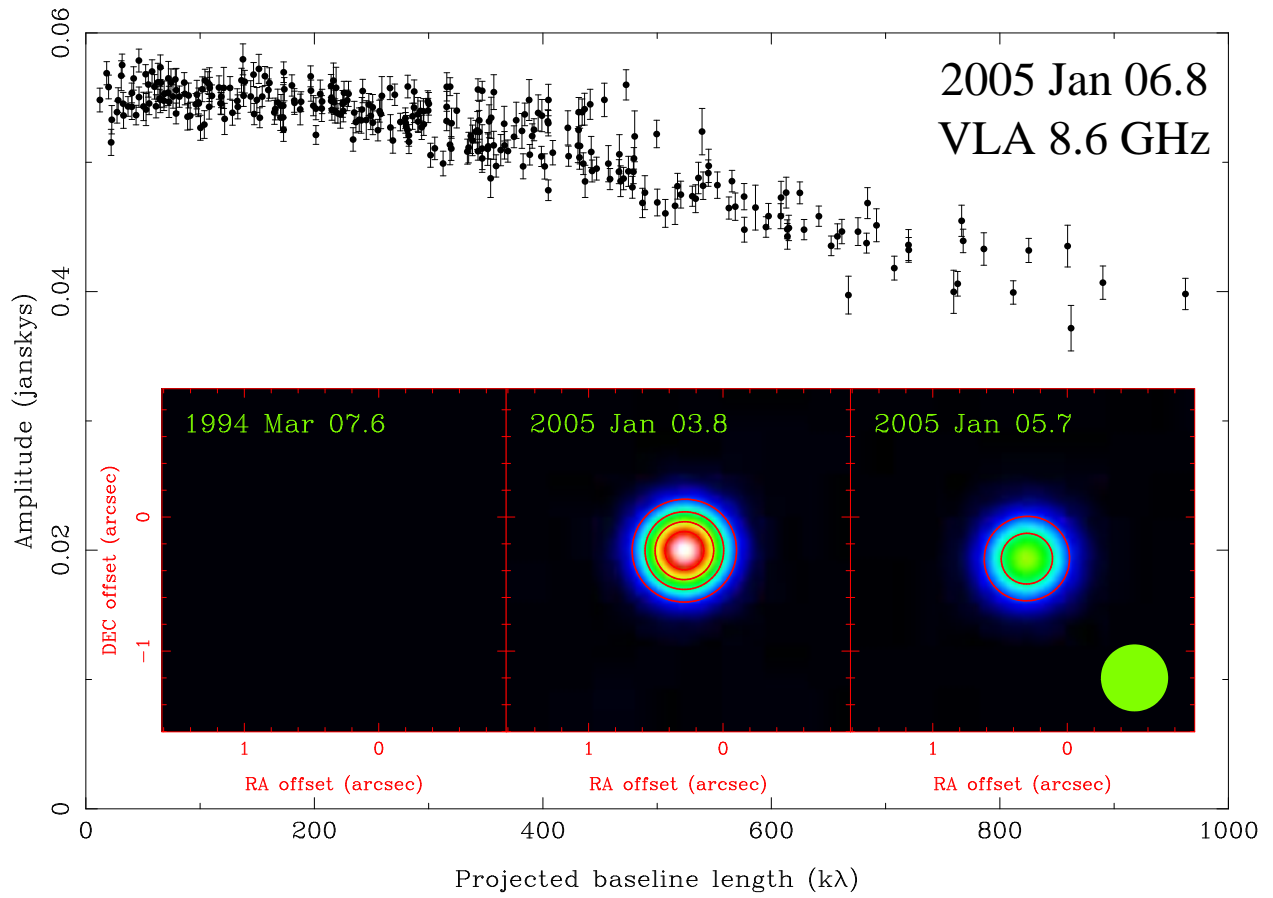


Figure 1.

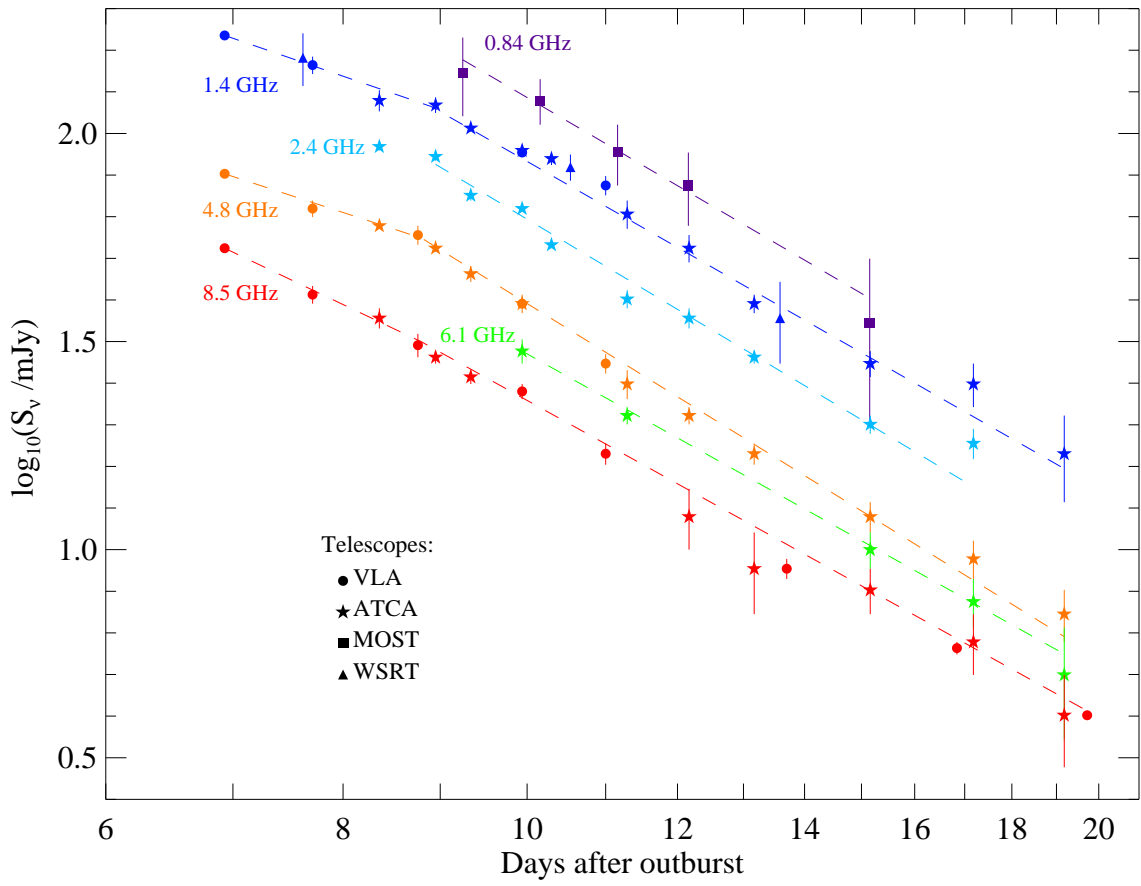


Figure 2.

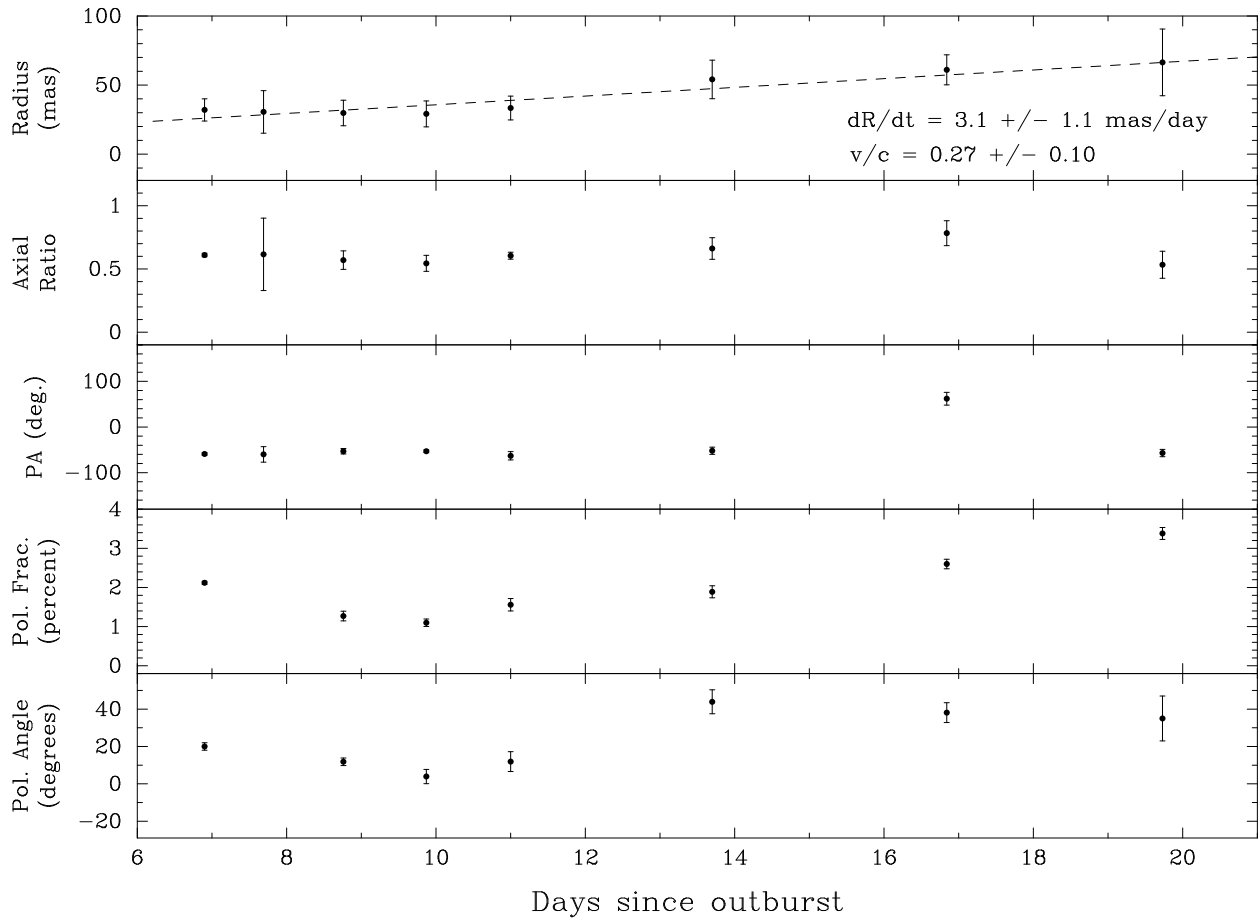


Figure 3.

SUPPLEMENTARY METHODS

Table 1. Flux density of VLA J180839–202439, the transient radio source coincident with SGR 1806–20, as a function of both time and frequency, as measured by the VLA, ATCA, WSRT and MOST. The epoch of the flare was 2004 Dec 27.89 UT. Uncertainties in each flux measurement are given at the $1\text{-}\sigma$ level. All telescopes carried out interferometric synthesis imaging of the field of SGR 1806–20 to make these measurements. The absolute flux scales were set using bright standard calibrators; on several days, different telescopes observed the source near simultaneously and obtained near identical flux measurements, indicating the reliability of this calibration. Phase calibration was carried using regular observations of nearby bright compact sources. At times when VLA J180839–202439 was bright enough, self-calibration in phase only was also applied. The data were then Fourier transformed to the image plane, deconvolved using the point response derived from the synthesis transfer function, and then convolved with a Gaussian beam corresponding to the diffraction limited resolution. Fluxes were then extracted in three ways: by integrating the surface brightness of the source, by fitting the image of the source to a Gaussian, and by modelling the source as a Gaussian in the complex visibility plane — results for total fluxes were consistent among these three approaches. The data with lower spatial resolution (most notably the MOST and WSRT observations) suffered from confusion from the bright radio source VLA J180840–202441 [Vasisht, Frail & Kulkarni, 1995, *The Astrophysical Journal (Letters)*, **440**, L65; Frail, Vasisht & Kulkarni, 1997, *The Astrophysical Journal (Letters)*, **480**, L129], $14''$ to the east of SGR 1806–20, associated with the Luminous Blue Variable (LBV) 1806–20 [Hurley et al., 1999, *The Astrophysical Journal (Letters)*, **523**, L37]. For these data, difference imaging and background subtraction were carefully applied to extract the radio flux of the transient source. The estimated uncertainties account for the systematic effects associated with this approach.

Mean Epoch (UT)	Days after Flare	Telescope	Flux Density (mJy)					
			0.84 GHz	1.4 GHz	2.4 GHz	4.8 GHz	6.1 GHz	8.5 GHz
Jan 03.83	6.93	VLA	...	172±4	...	80±1	...	53±1
Jan 04.52	7.62	WSRT	...	152±22
Jan 04.61	7.71	VLA	...	146±7	...	66±3	...	41±2
Jan 05.26	8.36	ATCA	...	120±7	93±2	60±1	...	36±2
Jan 05.66	8.76	VLA	57±3	...	31±2
Jan 05.85	8.95	ATCA	...	117±5	88±2	53±1	...	29±1
Jan 06.15	9.25	MOST	140±30
Jan 06.24	9.34	ATCA	...	103±2	71±2	46±2	...	26±1
Jan 06.85	9.95	ATCA	...	91±2	66±1	39±2	30±2	...
Jan 06.85	9.95	VLA	...	90±2	...	39±1	...	24±1
Jan 07.06	10.16	MOST	120±15
Jan 07.20	10.30	ATCA	...	87±3	54±1
Jan 07.44	10.54	WSRT	...	83±6
Jan 07.90	11.00	VLA	...	75±4	...	28±2	...	17±1
Jan 08.06	11.16	MOST	90±15
Jan 08.19	11.29	ATCA	...	64±5	40±2	25±2	21±1	...
Jan 09.06	12.16	MOST	75±15
Jan 09.07	12.17	ATCA	...	53±4	36±2	21±1	...	12±2
Jan 10.07	13.17	ATCA	...	39±2	29±1	17±1	...	9±2
Jan 10.49	13.59	WSRT	...	36±8
Jan 10.60	13.70	VLA	9.0±0.5
Jan 12.05	15.15	MOST	35±15
Jan 12.06	15.16	ATCA	...	28±2	20±1	12±1	10±1	8±1
Jan 13.74	16.84	VLA	5.8±0.2
Jan 14.08	17.18	ATCA	...	25±3	19±2	10±1	8±1	6±1
Jan 16.08	19.18	ATCA	...	17±4	...	7±1	5±2	4±1
Jan 16.62	19.72	VLA	4.0±0.1